ORIGINAL ARTICLE

In situ Imaging of Pea Starch in Seeds

Mary L. Parker · Andrew R. Kirby · Victor J. Morris

Abstract A method has been developed for the *in situ* imaging of starch in dry seeds by exploiting the tight packing of the starch and protein storage reserves within the cells of the embryo. The method can be adapted to prepare seed samples which are suitable for light microscopy (birefringence and iodine staining), scanning electron microscopy and atomic force microscopy. Its potential for imaging the internal structure of starch granules without any prior isolation process is demonstrated for round smooth peas. Using a standard ultramicrotome, thin sections were cut directly from selected regions of dry pea seeds and examined by light microscopy before and after hydration. The sectioning procedure left a planed surface with the internal structure of the starch granules exposed. This material was examined by scanning electron microscopy and atomic force microscopy directly or after controlled hydration. In the hydrated pea samples, the growth ring structure and blocklet sub-structure of individual starch granules within the seed were visualised directly by atomic force microscopy. Furthermore, the effects of hydration and staining were monitored and have been used to introduce contrast into the images. The observations have revealed new information on the blocklet distribution within pea starch granules and the physical origins of the growth ring structure of the granules: the blocklet distribution suggests that the granules contain alternating bands with different levels of crystallinity, rather than alternating amorphous and crystalline growth rings.

Keywords Starch · Pea starch · Atomic force microscopy · Light microscopy · Scanning electron microscopy · Starch granule structure

M. L. Parker · A. R. Kirby · V. J. Morris (✉)
Institute of Food Research, Norwich Research Park, Colney,
Norwich NR4 7UA, UK
e-mail: vic.morris@bbsrc.ac.uk

Introduction

A range of microscopic techniques can be used to probe the carbohydrate structure of starch granules. Light microscopy on intact granules provides information on granule size and shape. Differential contrast allows visualisation of the growth ring structure in hydrated granules and polarising optics reveals information on the orientation of crystalline structures within the granule. Confocal laser scanning optical microscopy (CSLM) has been used to study granular features such as protein content,[1] channels[2] plus cavities and growth rings.[3] Such methods can be used to probe the effects of starch structure on gelatinisation of the starch on heating.[3–5] Various staining procedures using iodine[4,6–7] or fluorescent labelling[8–9] can be used to locate amylose molecules and visualise the growth ring structure within the granule, for intact granules, or for sectioned material. Phosphate-binding dyes have also been used with CSLM to probe the distribution of phosphate in native granules.[9] The location of amylose in sectioned material can also be probed by immunolabelling methods.[7] Scanning electron microscopy (SEM) provides information on the shape and size of the granules and nature of the granule surface.[9–10] Transmission electron microscopy (TEM) of sectioned material has proved invaluable in visualising crystalline structure within granules and generating models of the overall molecular architecture of the starch granule.[11–12] Atomic force microscopy (AFM) provides a relatively new method for visualising the internal structure of starch granules.[13–20]

Recent TEM and AFM data[11–20] have led to renewed interest in the blocklet model of the starch granule.[12] High-resolution microscopy, using minimum perturbation of the granule structure, has allowed the demonstration of the presence of a level of starch granule organization

intermediate between that of the amylopectin crystalline lamellae and the large growth rings. These structural features involve the organisation of the amylopectin crystalline lamellae into packets or 'blocklets' which are embedded within an essentially amylose matrix.

An advantage of the use of AFM is that the information can be obtained with minimal preparation of the starches. To date, most studies have been made on starches isolated using a cycle involving wetting and drying. To visualise the internal structure the starches are encased in a non-penetrating resin and then cut open. Contrast in the AFM images is generated by controlled wetting of the cut faces or sections, which gives rise to localised absorption of water in selected regions of the granule. These regions swell and become soft providing the origin of contrast in the AFM images.[18,20] Embedding using resins that penetrate into the granule needs to be avoided because this leads to cross-linked structures that inhibit swelling on wetting sections or the cut faces of embedded material.[15–16, 21]

The ability to image the internal structure of starch directly within seeds would have several important advantages. Such a process would avoid the consequences of the cycle of hydration and dehydration during isolation of the starch. Such isolation procedures may alter the structure of the starch, or lead to selection of particular fractions of the granule population. These fractions may be unrepresentative of the starch granule population within the seed. By imaging the starch directly in the seed, the spatial distribution and heterogeneity of the starch granules within individual cells in different areas of the cotyledons are maintained. This information on heterogeneity is lost when the granules are isolated. The imaging of starch within individual seeds would also provide a basis for screening starch varieties for novel structures and for characterising any variability of intra- or inter-granule structure, arising from natural or induced mutations.

The established methods for preparing tissue samples for light and electron microscopy involve fixation, dehydration and embedding using organic solvents. For AFM studies, all of these stages can be avoided by exploiting the natural embedding of the starch within dry seeds. By producing very flat, clean surfaces of known orientation within the dry seeds using only standard electron microscopy (EM) sectioning procedures, it should be possible to produce ideal samples for AFM. The method should then allow controlled hydration of the samples to generate contrast within AFM images. By adapting this methodology for a range of microscopic methods and integrating the resulting images, a composite picture of starch structure within the seed should be achievable.

This article describes the development and use of such methodology to image starch structure within seeds. The methods will be illustrated for AFM, light microscopy (including birefringence and iodine staining), and scanning electron microscopy studies on round peas.

Materials and Methods

The methodology was tested using a range of round green pea seeds including Meteor (garden pea), Maro (marrowfat pea), and dried green peas from catering packs.

Sample Preparation for AFM

The testa was removed from the dry peas and a slice, approximately 2 mm thick, was sawn from the midpoint of each pea across the radicle using a fine-toothed saw. The two adpressed cotyledons in this slice were separated and blocks of tissue, approximately 3 mm wide, and including the whole thickness of the cotyledon from the upper to lower epidermis, were cut from the cotyledons. These blocks were glued with the transverse orientation of the cotyledon uppermost onto small squares of mica. The mica containing the sample was then attached to an aluminium SEM stub using a double-sided tab.

The stub was inserted into the chuck of an ultramicrotome (Reichert Ultracut E) and the surface tissue of the sample was planed away with a glass knife until a polished mirror-like surface was obtained. The mica was then split and the sample was transferred to a glass slide for AFM studies. When the seeds are cut open the exposed faces will absorb moisture from the atmosphere. This was usually insufficient to generate sufficient contrast for AFM studies. To introduce contrast for the AFM studies (and for the SEM samples), a wetting step was devised: water was boiled in a beaker and the steam was blown, or wafted across the face of the samples in a controlled procedure, in order to wet and hydrate the surface. By controlling the time of exposure to the steam it was possible to vary the degree of absorption and the subsequent swelling of the exposed faces of the cut seeds. The steam simply provides a source of moisture for varying the humidity above the surface of the sample: there is no localised heating of the sample. This additional 'minimal wetting' step was sufficient to generate contrast visible in the SEM and AFM without grossly hydrating and swelling the matrix surrounding the starch in the seeds.

Atomic Force Microscopy

AFM images were obtained on a Thermomicroscopes Lumina combined AFM/SNOM system and also on an Asylum MFP 3D. On the Lumina the planed faces of the seeds were scanned in air using the 'dry-scanner attachment'. Topographic and error signal mode images were generally obtained by scanning the cut faces in air in the dc

contact mode at a scan rate of 3 Hz, using narrow silicon nitride cantilevers with a nominal force constant of 0.38 Nm^{-1}. For some of the low-resolution images, where the cut faces were relatively rough over the scan sizes used, Mikromasch SC 12 type 'E' cantilevers with a nominal force constant of 0.30 Nm^{-1} were used. These cantilevers are normally employed in the non-contact mode. They are useful for low-resolution studies on comparatively rough samples because the tip height is of the order of 15 μm. However, the long length of the cantilevers (~ 300 μm) means that their sensitivity is low. For the Asylum MFP 3D the cut faces were scanned in air in Tapping mode using OMCL-AC160TS cantilevers at a set point of 0.63 V, a 1 Hz scan rate and a drive frequency of 336.3 kHz.

Light Microscopy

Sections (nominally 1–1.5 μm thick) of cotyledon tissue produced during the preparation of AFM samples were picked up with fine tweezers and mounted in light paraffin oil, or water, or dilute iodine/potassium iodide for examination using the bright field or polarising optics of an Olympus BX60 microscope. Images were recorded using Acquis (Syncroscopy, Cambridge) image acquisition software.

Scanning Electron Microscopy

Freshly prepared polished cotyledon surfaces, and similar samples 'minimally wetted' as described for the AFM studies, were sputter coated with a thin layer of gold (Emitech K550, Ashford) and examined in a Leica Stereoscan 360 scanning electron microscope at 10 kV. For comparison, fractured cotyledon material obtained by briefly immersing dry peas in liquid nitrogen before cracking them with a sharp blow, were also gold coated and examined by SEM as above.

Results

The SEM images of the fractured material (Figure 1a) are typical of pea starch[10] and show the compact arrangement of the starch, protein bodies and cell walls. The fracture has followed the boundary of the starch granules, the weakest plane in the cells of the dry pea. The three-dimensional spheroidal shape of the starch granules (s) is revealed by the projections of parts of the granule out of, or the depressions left in the fractured surface. The images also show the smaller tightly packed, angular protein bodies (pb), either as projections or depressions in the cytoplasm at the sample surface. Finally, in the dehydrated state the cell wall (cw) is thick, corrugated and compacted with intracellular spaces (ics) clearly visible. These same components are easily identified in low-resolution SEM images of the planed faces of the pea seed interior (Figure 1b). The outline of individual cells, the cell walls, starch grains and protein bodies are visible although some loose cell debris accumulates in the intercellular spaces during preparation. A few of the small starch granules are seen to have been plucked from the surface but not in

Fig. 1 Scanning electron micrographs of dry mature round pea seeds. **a** Cotyledon cells, fractured after freezing in liquid nitrogen, showing the tight packing of the starch granules and protein bodies. **b** Cotyledon cells planed smooth with a glass knife for AFM imaging. All of the starch granules have been cut open to expose their internal structure. **c** The internal structure of both large and small starch granules in planed seeds is featureless in the SEM, but the outlines of the surrounding protein bodies are evident. **d** For the first time it has been possible to observe the effects of minimal wetting of the surface of dry planed starch which allows differential expansion of the internal concentric rings (*arrow*); *cw* cell wall, *ics* intercellular space, *pb* protein bodies, *s* starch granule
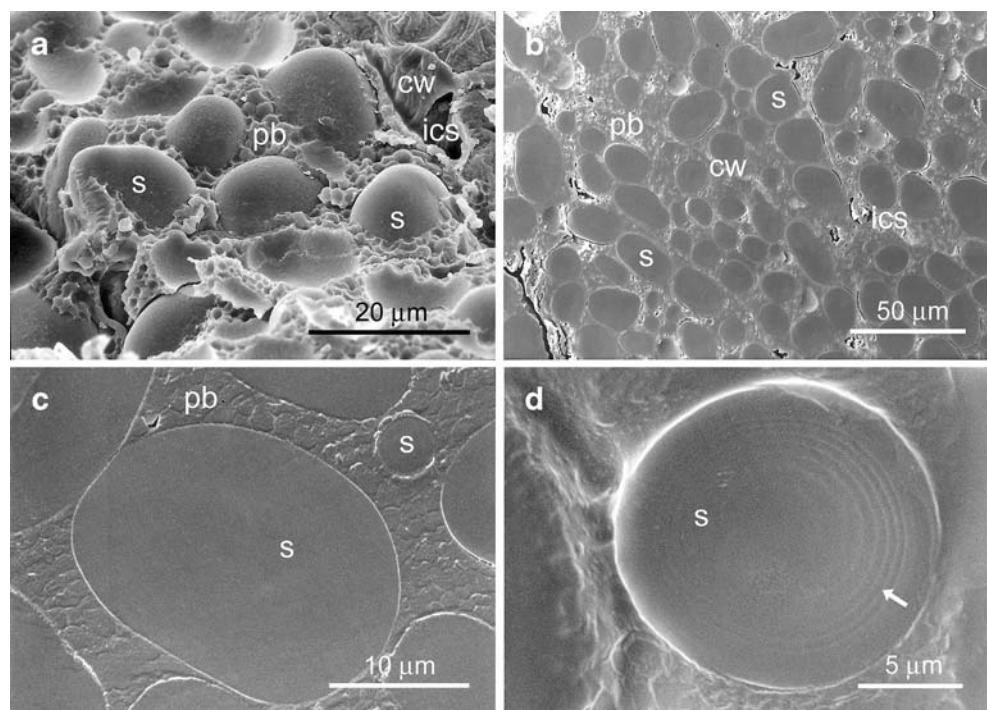
sufficient numbers to cause problems with imaging the planed faces by AFM. For granules cut through their central region, the axial ratio appears to be ∼2–1. The profiles of these starch granules within the seed suggest that their maximum size dimensions, determined from measurements on granules where the hilum is visible, are in the range 5–30 μm. These values are typical for those reported for isolated smooth pea starches.[10] From these images it is possible to select particular cotyledon cells and starch granules to be imaged by AFM. At higher magnification (Figure 1c), the outlines of the protein bodies surrounding the starch granules can be seen. Although the profiles of the starch granules are distinct, the exposed faces are featureless: no internal structures such as growth rings are visible in the large or small granules illustrated. In contrast, in the SEM images of the 'minimally hydrated' sample (Figure 1d) the minimal wetting of the sample results in the slight projection of each granule profile from the sample surface and the appearance of growth rings (arrowed) in some regions of the exposed faces of some of the granules. Where growth rings are seen they tend to be located at the outer regions of the granule. Visualisation of these features in the SEM must result from variations in height across the exposed part of the internal structure of the granule, as a consequence of selective absorption of water and irreversible swelling of these newly hydrated regions. Although some degree of sample dehydration during sputtering coating and in the higher vacuum of the SEM is to be anticipated, the height fluctuations across the surface have been preserved.

Thus these studies confirm that the topography induced by wetting the exposed surface of the granule is due to swelling of selected regions of the granule. As will be shown later the height variations induced on wetting are very small (∼ 12 nm) and therefore not easy to image in the SEM: observation of growth rings is the exception rather than the rule.

Light microscopy of the thin planed sections mounted in oil provides the closest approach to the observation of the native structure within the dry seed. In the low magnification image (Figure 2a) the cell wall (cw), protein bodies (pb) and starch granules (s) are easily identified. At higher magnification, the transparency of the thin section allows the location of chlorophyll (between arrows) to be identified in the green regions at the periphery of the starch granules (Figure 2b), and there is a characteristic 'pinched' structure in the central hilum region of the granules (Figure 2c and d) rather than a void. Differential interference contrast (Figure 2a) and polarisation studies (Figure 2d) of the granules within the seed reveal characteristic Maltese cross patterns, indicating radially aligned crystalline structures within the granules and confirming the lack of central voids in starch in dry seeds. Those slices which show the brightest Maltese crosses under crossed polarisers are those slices through the middle of the granule where the optic axes are most closely aligned with the incident polarised light. The growth rings are just visible within the birefringence patterns (Figure 2d). These images suggest that the growth rings represent bands within

Fig. 2 Thin planings of dry round pea mounted in oil for light microscopy. **a** Differential interference contrast image of dry cotyledon cells showing the close packing of starch (*s*), protein bodies (*pb*) and cell walls (*cw*). **b** Brightfield detail of the starch granules showing peripheral location of chlorophyll (*between arrows*). **c** Brightfield detail of starch from Maro pea showing chlorophyll (*between arrows*) and pinched central hilum area. **d** Polarised light micrograph of starch in Maro pea showing the concentric layers and pinched hilum with no central void
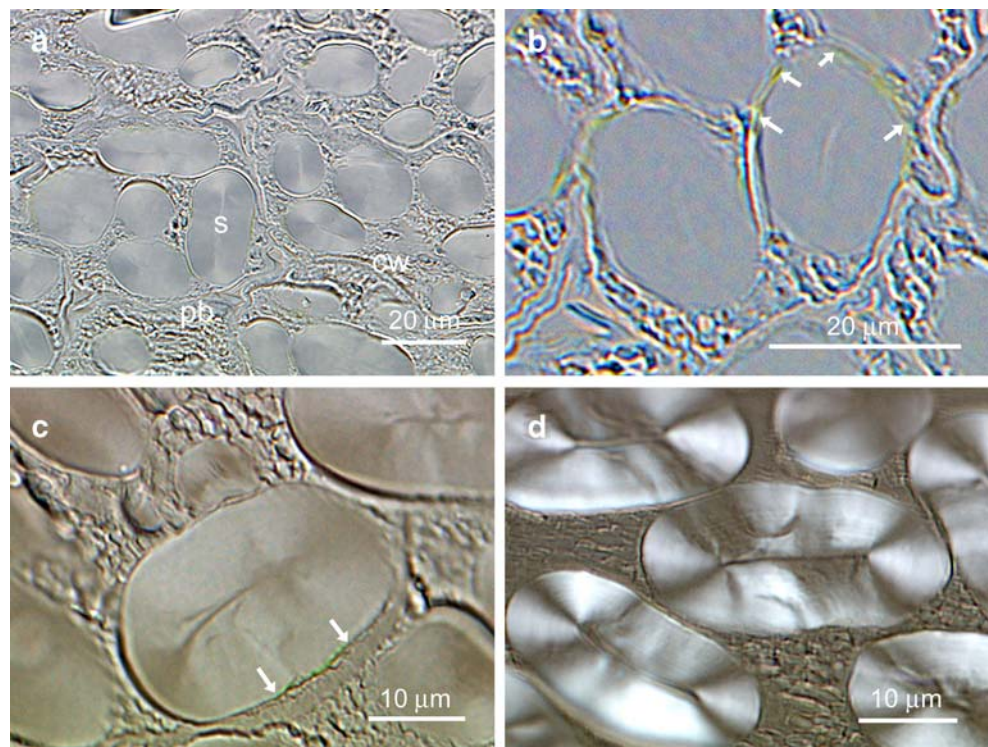
the granule in which the relative concentrations of the polysaccharide, and hence the refractive indices, are different. This would be consistent with alternating bands containing different levels of semi-crystalline starch poly-saccharides or either alternating amorphous and semi-crystalline rings. Thus, these observations alone cannot distinguish between the two presently accepted but different models of the starch granule structure: the alternative models correspond, respectively, to the blocklet model[12,16–20] of starch structure, derived from transmission electron microscopy (TEM) and AFM studies, or the more widely accepted structure used for modelling the small angle X-ray scattering (SAXS) data on starch.[22–28]

When the planed sections are mounted in water they immediately begin to hydrate and swell. Water is taken up in the protein bodies and cytoplasm, the cell wall, and sectioned starch, and the central 'pinched region' of the granules expands to form the distinctive hilum region (Figure 3a) sometimes with a crack-like void. The growth ring structure can be seen in the polarised light image of the same section (Figure 3b) and wetting has enhanced the contrast sufficiently to enable the growth rings to be visible directly in the polarised light image (Figure 3c). The latter images suggest that wetting has enhanced the difference in refractive index between the 'light' and 'dark' rings and this is consistent with the suggested preferential absorption of water within certain regions of the exposed faces of the starch granules.[18,20] It is noticeable that the growth rings

are seen in the outer regions of the granules and not in the central region.

In Figure 3d the effects of iodine staining can be observed. The dilute iodine/potassium iodide stain has been added at the top right-hand edge of the section, and allowed to spread across the section. In Figure 3d some of the starch granules have already taken up the iodine whilst some have yet to stain. By observing the staining activity as it passes across the section, it can be seen that the staining pattern in the starch is not homogeneous. Because the starch is in the form of thin sections, the iodine is able to access all parts of the granule directly, rather than diffusing from the outside inwards as in whole granules. The central region of the granule takes up stain less readily, suggesting some difference of structure within this region. As the staining intensifies, the growth ring structure is emphasised suggesting that alternate rings take up stain more easily than the neighbouring rings. Again, this would be consistent with the idea that certain rings are more hydrated making them more accessible to staining. If the level of staining is considered to be proportional to the amylose concentration, then the differential staining of the exposed faces of the granules could be taken to suggest that the amylose concentration is lower in the centre of the granule, and fluctuates over the region where the growth rings are visible. The advantage of using thin sections in the present study is the ability to resolve clearly these transient differences in internal staining pattern.


Fig. 3 Thin planings of dry round pea mounted in water for light microscopy. a Planings expand rapidly in water as the cell contents hydrate. b Same section as in a but viewed by polarised light to show the characteristic Maltese cross pattern in the starch granules. c Polarised light micrograph of starch granules showing details of the concentric rings and the open hilum. d Sections of starch granules stain readily with io-dine/potassium iodide but from the direction of the iodine ap-plication (arrowed) rather than centripetally as in whole granules
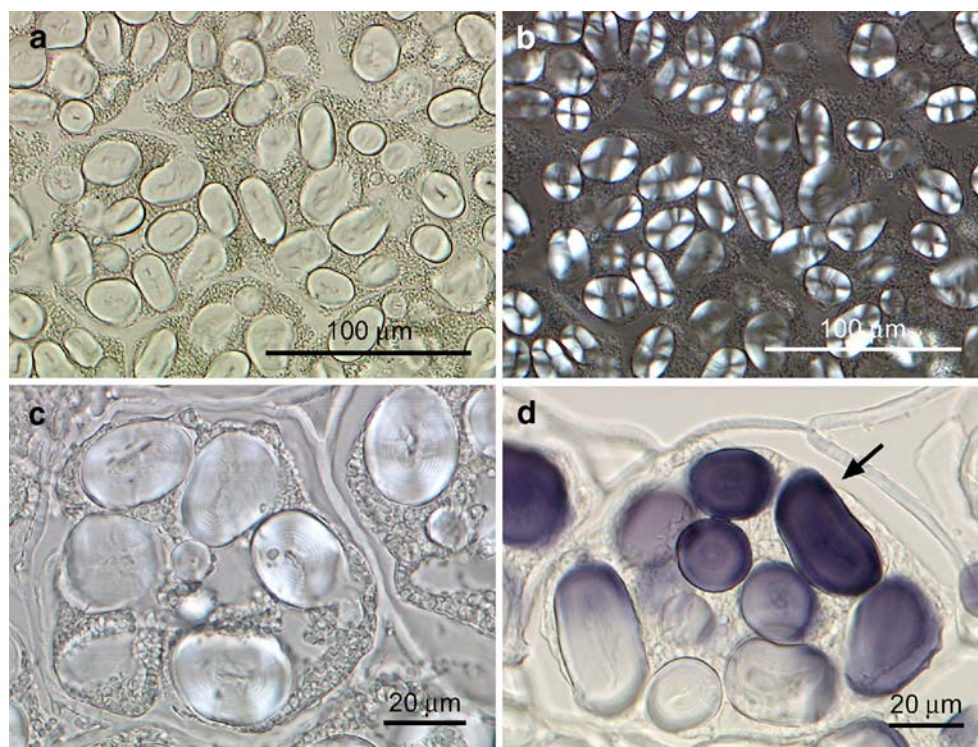
Even in the planed interior faces of the dry seeds it is possible to recognise different features in the AFM images. These can be identified by reference to the SEM and light micrographs of the material (Figures 1, 2, 3). The cell walls (cw), angular protein bodies (pb) and cut faces of the starch granules (s) can be seen in the low-resolution topographic AFM images shown in Figure 4b, d and f. These features are easier to see in the error signal mode images (Figure 4a, c and e) than in the topography or height images. It is perhaps surprising that the variation in contrast between the different components is so apparent, given that the cut faces are quite smooth. In both the AFM (Figure 4) and SEM images (Figure 1b and c) the main factor determining contrast in dry seeds will be variations in height across the

planed surface. Cutting open the seed will expose the cut faces to ambient humidity. Rapid uptake of moisture from the air will assist areas compressed during the dehydration stage of seed maturation to expand, and the differential expansion of the starch, protein bodies and cell walls is probably the main origin of contrast in both sets of images. In the AFM images, additional contrast may result from the different compressibility of the components within the seed. For the starch, it is noticeable that the outer regions of the exposed faces of the granule expand more than the central regions, perhaps indicating the release of internal stress when the dry starch granules are cut open. However, although the starch granules can be visualised there are no internal features visible within the granules in these images.

Fig. 4 AFM images of the cut faces of dry pea seeds. **a** Error signal mode image and the corresponding topography image **b**. The starch granules, cell wall and protein bodies are recognisable from the labelled regions in Figure 1. The image sizes are 80 × 80 μm. **c** Error signal mode image and the corresponding topography image **d**, image size 50 × 50 μm. **e** Error signal mode image and the corresponding topography image **f**, image sizes 20 × 20 μm. No internal structures are visible on the exposed faces of the granules
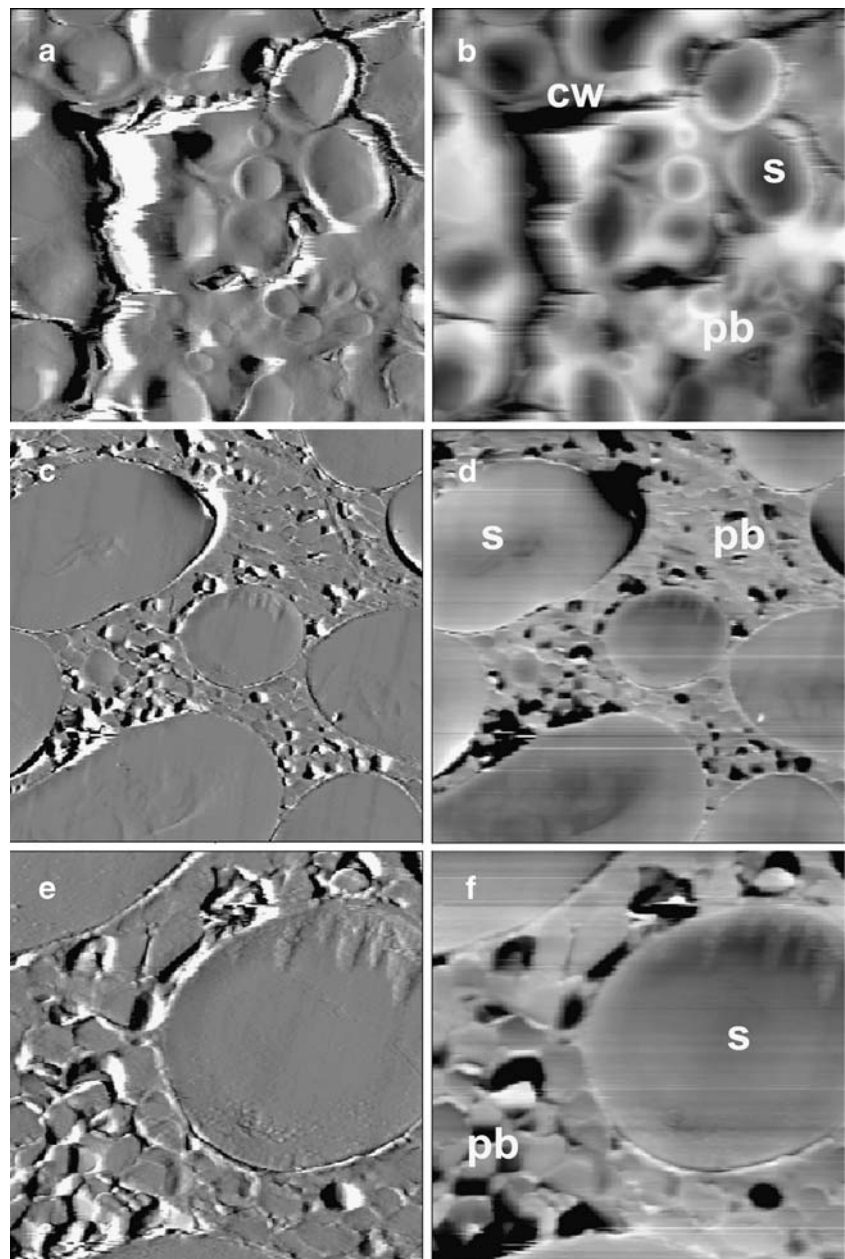
In previous studies of isolated, encased starch granules, it was necessary to wet the cut face to induce contrast, and to reveal the internal structure of the granule. The contrast was attributed to the selective absorption of water within different parts of the exposed face of the granule.[18,20]

In the previous studies[18,20] on encased starch, wetting was achieved by depositing a drop of water onto the cut surface and then removing excess water by capillary action using a filter paper. For the cut internal faces of the smooth pea seeds in the present study, this approach results in significant swelling of the cytoplasm and protein bodies, making the samples too rough to image by AFM. To reduce this effect, we have used a 'minimal wetting' process. By wafting steam across the cut surface, sufficient water is adsorbed by the starch to induce contrast, without causing excessive swelling of the other components. In the low-resolution images (Figure 5) of these wetted samples, it can be seen that the absorption of water has caused the cell wall region to expand and the protein bodies to swell and become rounded (Figure 5a and b). The outer regions of the granule are seen to expand more than the central region suggesting that the uptake of water is higher in the outer extremities of the granule. The growth ring structure of the starch granules becomes visible in the electronic image, but the contrast is small and difficult to discern in the printed images. At higher resolution (Figure 5c and d) the growth

ring structure is clearly visible, particularly in the error signal mode image (Figure 5c). In the topography image (Figure 5d) the height variation across the growth rings is ~12 nm. This small variation in height explains the difficulty in seeing the growth rings in the 'minimally wetted' samples by SEM. In Figure 5c, the upper left hand corner of the image shows the region close to the hilum. It can be seen that there is restricted swelling in this region and the growth rings are absent in the centre of the granule. As can be seen in the topographic image this region appears dark indicating restricted swelling (Figure 5d). The restricted swelling at the centre of the granule was noted in previous reports on the AFM of isolated, encased pea starch granules.[18,20] The present observations suggest that the structure of the granule in the central region, close to the hilum, is different from the structure in the outer region of the granule. This is supported by the observation that, in the birefringence images of the dry sections of the seeds in oil, the growth rings are not visible near the centre of the starch granules. Furthermore, in the dry samples, there is a pinched structure at the centre of the granules. In the wetted thin sections, there is also an absence of growth rings near the hilum, seen in the SEM and AFM images of the granules, and the nature of the hydration and iodine staining near the hilum also suggest that the granule structure is different at the centre, when compared to the

Fig. 5 AFM images of minimally-wet cut faces of pea seeds. a Error signal mode image and the corresponding topography image b. The starch granules cell wall and protein bodies are recognisable from the labelled regions in Figure 1. The image sizes are 20 × 20 μm. c Error signal mode image and the corresponding topography image d, image size 4.7 × 4.7 μm. Wetting has revealed the growth ring structure and some detail of substructure within the growth rings
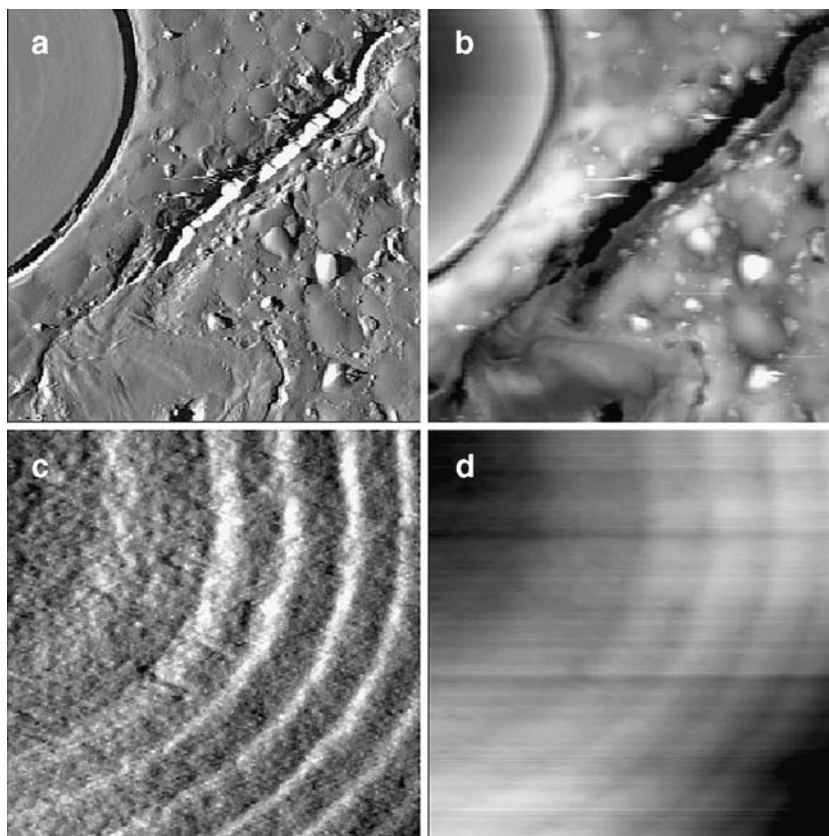
surrounding region, where the growth rings are seen. A plausible explanation is that the amorphous amylose preferentially absorbs water and that the amylose concentration increases from the centre towards the outer boundaries of the granule. Furthermore, the existence of the growth rings would suggest that the amylose concentration fluctuates periodically across the outer regions of the granule where the growth rings are seen.

Some degree of substructure is just visible within the growth rings (Figure 6a and b) in higher resolution AFM images. Detail is easier to see in the error signal mode image (Figure 6a) than in the topography image (Figure 6b). Shading of the topography image (Figure 6c) reveals more detail on the height variation across the image. As reported previously, it was possible to visualise the substructure within the growth rings in wetted, encased cut faces of isolated starches.[18–20] In the present studies, the higher resolution images of the minimally wetted seeds reveal more detail on the internal substructure of the granule when obtained using the Asylum MFP 3D (Figure 7) than with the VEECO Lumina apparatus (Figures 5 and 6). The VEECO Lumina apparatus is a first-generation combined AFM-optical microscope, and the scan size and resolution is limited. Modern combined optical-SPM microscopes incorporate, rather than just add, the AFM to the inverted optical microscope. This means that these new microscopes have considerably enhanced mechanical rigidity over the previous generation equipment and produce superior images. Figure 7 shows higher resolution AFM images of the minimally wetted, exposed faces of starch granules, within the planed face of the pea seed, obtained using an Asylum MFP 3D apparatus. The growth ring structure and the substructure within the growth rings are clearly visible, even in the topography images. As seen previously,[18,20] for AFM images of isolated starches, the presently-observed growth rings

consist of bright swollen bands, interspersed by dark largely unswollen regions. The darker 'bands' are incomplete, and consist of a series of dark, relatively unswollen patches (Figure 7a and c). Round structures, previously attributed to blocklets, are seen within the swollen regions of the granule. The most convincing TEM evidence for blocklet structures in starch granules arises from the use of the PATAg method.[12] This mild oxidation treatment leads to a localised staining of the amorphous regions within the granule due to the accumulation of silver within these regions. In the present AFM studies, the contrast between amorphous and crystalline regions within the granule is attributed to the preferential swelling of the amorphous regions. This localized swelling would account for the localization of staining by the PATAg method. Oxidation would preferentially occur in the hydrated regions and hence a mild oxidative treatment would be largely confined to the amorphous regions of the granule. Hence, it is suggested that the round objects revealed in the AFM images correspond to the blocklets identified from the TEM studies.

The dark patches are largely unswollen and it is not possible to visualize any substructure within these regions in the topographic (height) images (Figure 7b and d). The limited swelling achieved by controlling the wetting process, ensures that the exposed cut faces of the starch granules remain relatively flat: the maximum height variation across the starch granules shown in Figure 7b and d is only 12 nm. Thus, the equivalent phase images, shown in Figure 7a and c, can be used to assess the relative hardness of the bright and dark regions within the granule. In the phase images, the round 'blocklets' appear darker, which is also consistent with hard semi-crystalline objects suspended in a softer matrix (lighter) region. Throughout the imaging process the phase angle remains below 80°, suggesting that the imaging conditions remain in the
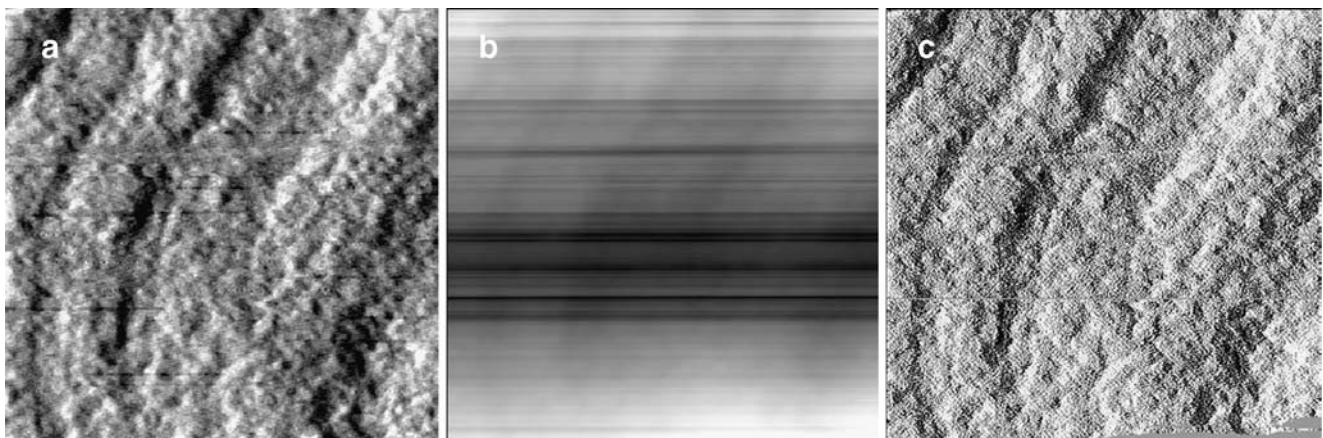

Fig. 6 AFM images of the minimally-wetted cut face of a pea starch granule within a pea seed, image size 3.8 × 3.8 μm. **a** Error signal mode image, **b** topography image and **c** left-shaded topography image. These images reveal substructure within the growth rings. This is most evident in the error signal mode image **a** but detail is difficult to see in topography images **b** unless they are shaded to emphasise changes in height **c**
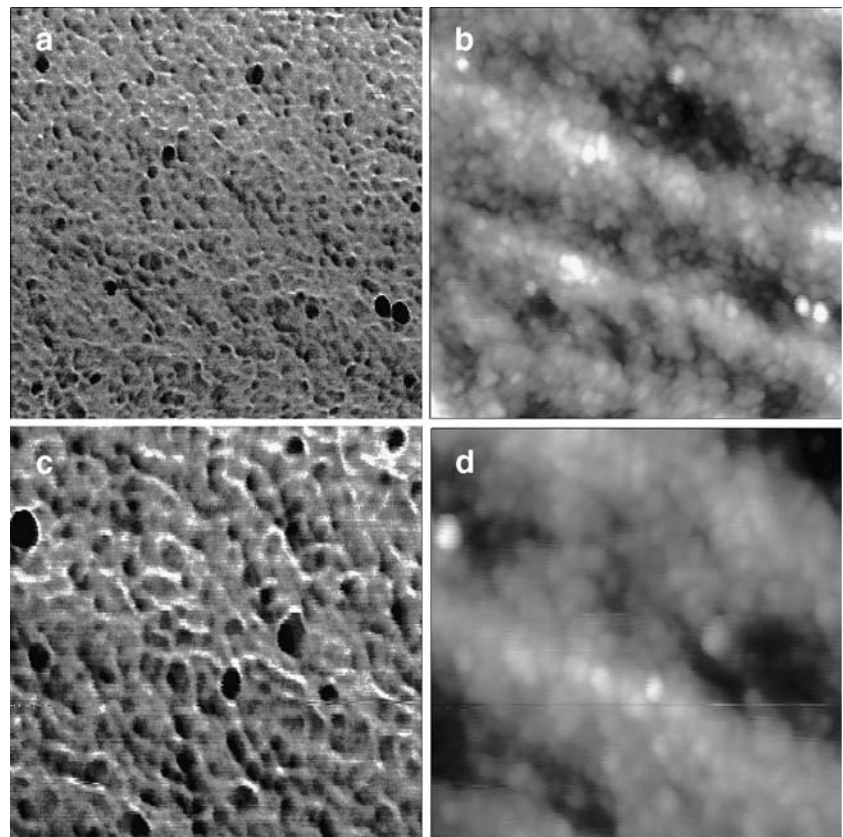
Tapping mode, and the fluctuations in phase are not due to switching between Tapping and contact mode, as a consequence of any height variations on the sample surface: the transition between Tapping and contact mode is normally considered to occur at 90°. The phase images (Figure 7a and c) also reveal a substructure, or blocklet structure within the dark, relatively unswollen patches in the dark bands (Figure 7b and d). Although the matrix surrounding the blocklets in the dark patches does not swell sufficiently to allow the blocklets to be visible in the height images, this matrix region does appear to absorb water and become softer than the blocklets, allowing the blocklets to be seen in the phase images. This is consistent with previous suggestions that water is preferentially absorbed in the amylose matrix surrounding the semi-crystalline, amylopectin-based blocklets. Furthermore, it supports the suggestion that the dark patches may swell less because they contain smaller amounts of amylose. These images support the granule structure suggested by Gallant and co-workers.[12] Blocklets are seen in both the bright and dark bands suggesting that both are semi-crystalline. In the Gallant and co-workers model[12] the schematic picture suggests that the blocklet size is different in the two bands. In the current images the blocklet size appears to be the same in alternate bright and dark bands. The banding structure appears to arise from the presence of isolated patches within the dark bands which swell less than the surrounding material. The phase images allow the blocklet substructure within these patches to be visualized for the first time.

Discussion

The current detailed models of starch ultrastructure are based on the cluster model of the starch granule deduced from the modelling of SAXS data.[22–28] However, it has been difficult to obtain direct experimental evidence in support of this model. Our experimental evidence, in the form of SEM and AFM images, suggests that the starch granules contain alternating layers (growth rings) containing different degrees of semi-crystalline material.[12,16–20] Within the growth rings, it is suggested that the crystalline lamellae, formed from the branches of the amylopectin molecules, are packaged into blocklet structures, which themselves reside in a matrix of amorphous amylose. At present the TEM and AFM methods describe the long-range structures within individual granules and only with the TEM has it been possible at present to resolve the individual crystalline lamellae.[12] The SAXS data will provide information on the detailed molecular structure within the alternating crystalline and amorphous lamellae

formed by the branched 'amylopectin' structures within the granule. This scattering pattern will be modified by the details of the growth ring structures. The measured scattering pattern will be averaged over all orientations of the granule and all sizes and shapes of the granule population. In the original Gallant and co-workers'[12] description of the blocklet structure of the granule, it was suggested that the crystalline and amorphous lamellae formed by the branched 'amylopectin' structures are contained, or packaged within the blocklets. Furthermore, the TEM and AFM data suggest that there are no true amorphous growth rings within the granules, only alternating layers with different refractive indices (different electron densities). Thus, the major differences between the models are the detailed nature of the growth rings and whether or not the alternative crystalline and amorphous regions, formed by the branched 'amylopectin' structures, are packed into discrete units (blocklets) contained in an amorphous matrix. It is still difficult at present to visualise the molecular structure within the blocklets by either TEM or AFM.

At present the two models of the starch granule are not contradictory but complementary. One route to reconciling the two models might be to introduce a particulate (blocklet) organisation and modified growth ring structure into a thus more heterogeneous model of the SAXS data.

The methodology developed for AFM imaging of starch directly within dry peas has been shown to be adaptable and compatible with SEM and light microscopy studies. One of the main advantages conferred by the inclusion of a novel mica mount in the preparation stage, is the ability to transfer material between the microtome and the AFM and SEM stages whilst maintaining the known orientation of the sample. The effects of controlled hydration can be monitored and used to generate contrast in both the AFM and SEM. The section planings obtained during the polishing step can be used for conventional light microscopy, iodine staining and birefringence studies. The technique of dry sectioning has been used previously to locate protein deposits in wheat grains,[29] but the method described here is more versatile and has considerable potential for further *in situ* studies of starch structure. When sections are imaged in oil, the native state of the water-soluble components, such as chlorophyll, can be readily identified. When mounted in water, the progressive uptake of iodine into different regions of the starch can be followed. The present observations are consistent with the theory that the amylose concentration varies throughout the granule and is responsible for aspects of the contrast observed in SEM, light microscopy and AFM at different levels of structural resolution. The methods used for iodine staining could be adapted for use with other stains, including the use of fluorescent methods to label starch polysaccharides at their reducing ends, and to map the distribution of amylose and

amylopectin within granules.[9] The sections mounted on barium fluoride discs are potentially suitable for Fourier transform infrared microscopy (FTIR). In addition, it may be possible to scan the sections with a synchrotron beam or produce sufficiently thin sections for subsequent studies by far-field or near-field infrared microscopy or TEM. The feasibility of FTIR studies on dry soybean seeds has been demonstrated recently by Miller and co-workers.[30] This would allow the mapping of the samples using a range of microscopic methods and possibly other techniques such as X-ray scattering or diffraction. Such physical studies on individual granules may ultimately provide a means of relating the heterogeneous structures seen by microscopy with the detailed molecular structure available from X-ray diffraction and scattering measurements.

Conclusions

A method has been developed for *in situ* AFM imaging of starch within dry seeds and is demonstrated for smooth pea. After controlled minimal wetting of cut internal faces of the seed, it has been possible to visualise the growth ring structure and blocklet sub-structure within the granules using a variety of microscopic methods. The methodology allows the effects of hydration and staining to be monitored and for hydration to be used to introduce novel contrast into the images. These studies have revealed, for the first time, that the blocklet structure is continuous throughout the granule. In the AFM images, the growth rings consist of bright (swollen) and dark (less swollen) bands, both of which are semi-crystalline. The dark bands are heterogeneous, consisting of patches of swollen and largely unswollen regions. It is proposed that the relatively unswollen patches are regions containing a lower concentration of amylose.

References

1. X.Z. Han, B.R.J. Hamaker, Association of starch granule proteins with starch ghosts and remnants revealed by confocal laser scanning microscopy Cereal. Chem. **79**, 892 (2002)
2. K.C. Huber, J.N. BeMiller, Channels of maize and sorghum starch granules Carbohydr. Polym. **41**, 269 (1997)
3. F. van de Velde, J. van Riel, R.H. Tromp, Visualisation of starch granule morphologies using confocal scanning laser microscopy (CSLM) J. Sci. Food Agric. **82**, 1528 (2002)
4. J.L. Jane, J.J. Shen, Internal structure of the potato starch granule revealed by chemical gelatinization Carbohydr. Res. **247**, 279 (1993)

5. T.Y. Bogracheva, V.J. Morris, S.G. Ring, C.L. Hedley, The granular structure of C-type pea starch and its role in gelatinisation Biopolymers **45**, 323 (1998)

6. A.G.J. Kuipers, E. Jacobsen, R.G.F. Visser, Formation and deposition of amylose in the potato-tuber starch granule are affected by the reduction of granule-bound starch synthase gene-expression Plant Cell **6**, 43 (1994)

7. N.J. Atkin, S.L. Cheng, R. Abeysekera, A. Robards, Localisation of amylose and amylopectin in starch granules using enzyme-gold labeling Stärke **51**, 163 (1999)

8. A. Blennow, M. Hansen, A. Schulz, K. Jorgensen, A.M. Donald, J. Sanderson, The molecular deposition of transgenically modified starch in the starch granule as imaged by functional microscopy J. Struct. Biol. **143**, 229 (2003)

9. M.A. Glaring, C.B. Koch, A. Blennow, Genotype-specific spatial distribution of starch molecules in the starch granule: a combined CLSM and SEM approach Biomacromolecules **7**, 2310 (2006)

10. W.S. Ratnayake, R. Hoover, T. Warkentin, Pea starch: Composition, structure and properties- a review Stärke **54**, 217 (2002)

11. G.T. Oostergetel, E.F.J. van Bruggen, The crystalline domains in potato starch granules are arranged in a helical fashion Carbohydr. Polym. **21**, 7 (1993)

12. D.J. Gallant, B. Bouchet, P.M. Baldwin, Microscopy of starch: evidence of a new level of granule organization Carbohydr. Polym. **32**, 177 (1997)

13. T. Ohtani, T. Yoshino, T. Ushiki, S. Hagiwara, T. Maekawa, Structure of rice starch granules in nanometre scale as revealed by atomic force microscopy J. Electron. Microscopy **49**, 487 (2000)

14. T. Ohtani, T. Yoshino, T. Ushiki, S. Hagiwara, T. Maekawa, High-resolution imaging of starch granule structure using atomic force microscopy Stärke **52**, 150 (2000)

15. A.A. Baker, M.J. Miles, W. Helbert, Internal structure of the starch granule revealed by AFM Carbohydr. Res. **330**, 249 (2001)

16. M.J. Ridout, A.P. Gunning, R.H. Wilson, M.L. Parker, V.J. Morris, Using AFM to image the internal structure of starch granules Carbohydr. Polym. **50**, 123 (2002)

17. M.J. Ridout, M.L. Parker, C.L. Hedley, T.Y. Bogracheva, V.J. Morris, Atomic force microscopy of pea starch granules: granule architecture of wild-type parent, r and rb single mutants, and the rrb double mutant Carbohydr. Res. **338**, 2135 (2003)

18. M.J. Ridout, M.L. Parker, C.L. Hedley, T.Y. Bogracheva, V.J. Morris, Atomic Force Microscopy of Pea Starch: Origins of Image Contrast Biomacromolecules **5**, 1519 (2004)

19. M.J. Ridout, M.L. Parker, C.L. Hedley, T.Y. Bogracheva, V.J. Morris, Atomic force microscopy of pea starch granules: granule architecture of the rug3 rug4 rug5 and the lam mutants Carbohydr. Polym. **65**, 64 (2006)

20. V.J. Morris, M.J. Ridout, M.L. Parker, AFM of starch: Hydration and Image Contrast Progr Food Biopolym. Res. **1**, 28 (2005)

21. W. Helbert, H. Chanzy, The ultrastructure of starch from ultrathin sectioning in melamine resin Stärke **48**, 185 (1996)

22. R.E. Cameron, A.M. Donald, A small angle x-ray scattering study of the annealing and gelatinization of starch Polymer. **33**, 2528 (1992)

23. D.R. Daniels, A.M. Donald, An improved model for analyzing the SAXS of starch granules Biopolymers. **69**, 165 (2003)

24. D.R. Daniels, A.M. Donald, Soft material characterization of the lamellar properties of starch: Smectic side-chain liquid-crystalline polymeric approach Macromolecules **37**, 11312 (2004)

25. A.M. Donald, K.L. Kato, P.A. Perry, T.A. Waigh, Scattering studies of the internal structure of starch granules Stärke **53**, 504 (2001)

26. T.A. Waigh, K.L. Kato, A.M. Donald, M.J. Gidley, C.J. Clarke, C. Rickel, Side-chain liquid-crystalline model for starch Stärke **52**, 450 (2000)

27. T.A. Waigh, P.A. Perry, C. Rickel, M.J. Gidley, A.M. Donald, Chiral side-chain liquid-crystalline properties of starch Macromolecules **31**, 7980 (1998)

28. J.S. Sanderson, R.D. Daniels, A.M. Donald, A. Blennow, S.B. Engelsen, Exploratory SAXS and HPAEC-PAD studies of starches from diverse plant genotypes Carbohydr. Polym. **64**, 433 (2006)

29. M.J. Wolf, U. Khoo, Mature cereal grain endosperm: rapid glass knife sectioning for examination of proteins Stain Technol. **45**, 277 (1970)

30. S.S. Miller, L.N. Pietrzak, D.L. Wetzel, Preparation of soybean seed samples for FTIR microspectrometry Biotechnic. Histochemistry **80**, 117 (2005)